Utah State University
DigitalCommons@USU

Space Dynamics Lab Publications | Space Dynamics Lab

6-30-2011

Model-Based Autofoceus for Stripmap SAR Images Formed via Convolution Back-Projection

Roger West

Jake Gunther

Todd Moon

Follow this and additional works at: https://digitalcommons.usu.edu/sdl_pubs

Recommended Citation
West, Roger; Gunther, Jake; and Moon, Todd, "Model-Based Autofoceus for Stripmap SAR Images Formed via Convolution Back-Projection" (2011). *Space Dynamics Lab Publications*. Paper 142.
https://digitalcommons.usu.edu/sdl_pubs/142

This Article is brought to you for free and open access by the Space Dynamics Lab at DigitalCommons@USU. It has been accepted for inclusion in Space Dynamics Lab Publications by an authorized administrator of DigitalCommons@USU. For more information, please contact dylan.burns@usu.edu.

UtahStateUniversity
MERRILL-CAZIER LIBRARY

West, Roger, Jake Gunther, and Todd Moon. 2011. "Model-Based Autofocus for Stripmap SAR Images Formed via Convolution Back-Projection." Paper presented at Tri-services Radar Conference, Monterrey, CA, June 27-30.

Approved for public release; distribution is unlimited

Model-Based Autofocus for Stripmap SAR Images Formed via Convolution Back-Projection

June 2011

Roger West, Jake Gunther, Todd Moon

Utah State University
Dept. of Electrical and Computer Engineering
4120 Old Main Hill
Logan, UT 84341

ABSTRACT

Many autofocus algorithms exist for correcting uncompensated residual phase errors in SAR images. These algorithms depend on the SAR modality (*i.e.* spotlight, stripmap, etc.). In this paper, we develop a model-based phase error estimation method and apply it to correct the phase error for stripmap SAR images formed via convolution back-projection (CBP). Our phase estimation method uses classical subspace fitting techniques well known in the array processing literature. The novelty in this paper is how we derive our autofocus method from the stripmap SAR forward model and we show that applying the phase error correction to the very popular CBP algorithm is very natural. We also show that our proposed method is non-iterative in the sense that we do not have to iterate between the image domain and the range compressed domain to obtain the phase error estimates. As our derivation shows, we do not have to form the image to estimate the phase errors.

1.0 Introduction

Despite the best efforts to have a synthetic aperture radar (SAR) sensor follow a predetermined nominal trajectory, phase errors still exist in the SAR data that corrupt the azimuth compression of the collected data. It is well known that these phase errors come mainly from two sources, [1-3]. A low frequency phase error will exist for uncompensated platform deviation, which has the effect of broadening the main-lobe of the azimuth compressed signals. Most of the gross platform errors are accounted for via motion compensation algorithms which use available navigational data. However, navigational data has limited accuracy and is corrupted by noise as well. The other source of phase error stems from signal propagation effects. These phase errors tend to be high frequency phase errors and the effect they have is not so much broadening the main lobe of the azimuth compressed pulse as raising the side-lobes, which lowers the contrast of the image and masks less reflective objects in the image. Autofocus algorithms are data driven algorithms that estimate and correct these phase errors.

Several autofocus algorithms exist, most of which are specific to the particular SAR modality being used (stripmap, spotlight, etc.). Each approach can be further classified as parametric, non-parametric, or metric based. The parametric approaches (such as mapdrift) tend to model the phase error as a polynomial or as sinusoidal and use the data to estimate the coefficients [2-5]. Because they use the data to estimate the coefficients, they are limited to only reliably estimating a small number of coefficients. Hence, these approaches perform well if the phase error is low frequency, but they fail to model the presence of high frequency phase error. The non-parametric approaches make the assumption that all of the range data collected from a single pulse is corrupted by the same phase error [2], [6-7]. If this holds, non-parametric techniques are able to estimate both low and high frequency phase errors. Finally, the metric based methods generally assume that the phase error has low frequencies and that it comes from a sensor velocity error. However, they can also be combined with non-parametric methods to produce good results, [8-9]. They utilize a cost function, such as image intensity or neg-entropy, to correct the azimuth matched filter that is applied to azimuth compress the data.

What all these methods have in common is that they must step back in the processing chain (usually azimuth decompression) to where the individual phase errors from each pulse exist to apply the phase compensation. For spotlight SAR, this amounts to computing an azimuth FFT to decompress the azimuth pulses, applying the phase compensation, then re-compressing in azimuth via an inverse FFT. Azimuth decompression is not quite so straightforward for stripmap SAR. The azimuth compression is accomplished by matched filtering. Deconvolving the azimuth matched filter to decompress the image and get back to the range compressed data is an ill-posed problem. Thus the range compressed data must be saved; this is the domain where phase error compensation must take place.

There are a variety of ways in which autofocus is implemented for stripmap SAR. This paper develops a novel model-based non-parametric autofocus method explicitly for stripmap SAR images that are formed using the convolution back-projection (CBP) algorithm.

This paper is outlined as follows. The phase error model is developed in section 2. The proposed autofocus method is derived in section 3. The gradient ascent optimization strategy is derived in section 4. A demonstration of the proposed autofocus method and gradient ascent is given in section 5. A discussion of the demonstrated results is given in section 6. Finally, conclusions are given in section 7.

2.0 Phase Error Model Development

In the CBP algorithm, we are interested in reconstructing the image to a predetermined reconstruction grid that has N_r range bins and N_a azimuth bins. Usually there is a digital elevation model (DEM) that accompanies the collected SAR and navigational data so the radial distance from the sensor location to each reconstruction point can be determined. Motion compensation due to gross sensor position deviations from the nominal trajectory are easily accounted for in the CBP algorithm, but unknown phase errors due to sensor location uncertainty, DEM errors, and signal propagation errors typically are not.

This section derives a model for the phase errors. We begin by stating a model for phase error free data and then show how to alter the model to include phase errors.

2.1. Phase Error-Free Model

In [10] a linear forward model was developed for stripmap SAR. The maximum likelihood (ML) image formation method stemmed from the interpretation of the forward model with additive noise as the linear statistical model. It was also shown that CBP is the first step in the ML image formation. Here we will use the same model for phase estimation. The linear forward model that was presented in [10] is

$$d(k,n) = \sum_{a,r} f(k,n,\boldsymbol{u}_{a,r},\boldsymbol{\theta}) g(\boldsymbol{u}_{a,r}) + \eta(k,n), \qquad (1)$$

where $g(\boldsymbol{u}_{a,r})$ is the ground reflectivity at the three dimensional ground location $\boldsymbol{u}_{a,r}$ in the a^{th} row and r^{th} column of the reconstruction grid, f is the point-spread response of the SAR sensor for the reflector at $\boldsymbol{u}_{a,r}$, $\boldsymbol{\theta}$ is a vector of SAR parameters such as the transmitted waveform, antenna pattern, etc., and η is circularly symmetric additive white Gaussian noise. In (1), $0 \le k \le N_k - 1$ indexes the transmitted pulses, $0 \le n \le N_n - 1$ indexes the samples taken from each pulse, $0 \le r \le N_r - 1$ indexes the columns of the reconstruction grid, and $0 \le a \le N_a - 1$ indexes the rows of the reconstruction grid.

The rows of the two dimensional array in (1) can be transposed and stacked to form an $N_n N_k \times 1$ vector $\boldsymbol{d}$. Similarly, f can be rearranged into an $N_n N_k \times N_r N_a$ matrix F, g can be rearranged into an $N_r N_a \times 1$ vector $\boldsymbol{g}$, and η can be rearranged into an $N_n N_k \times 1$ vector $\boldsymbol{\eta}$. The linear model can then be written as

$$\boldsymbol{d} = F\boldsymbol{g} + \boldsymbol{\eta}. \qquad (2)$$

The data matrix F can be decomposed into N_k, $N_n \times N_r N_a$ sub-matrices

$$F = \begin{bmatrix} F_0 \\ \vdots \\ F_{N_k-1} \end{bmatrix}, \qquad (3)$$

where the sub-matrix F_k models the expected returns from the ground locations under the illumination of the antenna based on all navigational data from the k^{th} pulse.

It was shown in [10] that the CBP image (in terms of (2)) is computed from the matrix/vector product

$$\begin{aligned} \boldsymbol{g}_{CBP} &= F^H \boldsymbol{d} \\ &= \begin{bmatrix} F_0^H \boldsymbol{d}_0 & \cdots & F_{N_k-1}^H \boldsymbol{d}_{N_k-1} \end{bmatrix} \mathbf{1}, \qquad (4) \\ &= G\mathbf{1} \end{aligned}$$

where $\boldsymbol{d}_k$ is the collected data from the k^{th} pulse and $\mathbf{1}$ is the vector of all ones.

If the $\mathbf{1}$ vector is replaced by a vector $\boldsymbol{\beta}$, where $\beta_k = e^{j\phi_k}$, then

$$\boldsymbol{g}_{CBP} = G\boldsymbol{\beta},$$

is a generalized CBP reconstruction. If phase errors did exist in the data, then the vector $\boldsymbol{\beta}$ could be found that corrects for the phase error, while simultaneously forming the CBP image.

2.2. Phase Error Model

If the incidence angle does not vary too much over the scene and the uncompensated phase error is not too large, then the model for the uncompensated phase error from the k^{th} pulse manifests itself as a constant phase multiplier for all the samples collected from the k^{th} pulse. (If the first assumption does not hold, data from a narrow strip (in range) of the reconstruction grid can be used so the assumption does hold.) The model for the uncompensated phase error from the k^{th} pulse is

$$F_k(\beta_k) = \Lambda_{\beta_k} F_k,$$

where $\Lambda_{\beta_k} = \beta_k I$ and $\beta_k = e^{j\phi_k}$ is the unknown phase term.

If a residual phase error exists for each pulse, the resulting model becomes

$$F(\boldsymbol{\beta}) = \Lambda_{\boldsymbol{\beta}} F, \quad (5)$$

where

$$\begin{aligned} \Lambda_{\boldsymbol{\beta}} &= \text{BlockDiag}\left(\Lambda_{\beta_0} \quad \cdots \quad \Lambda_{\beta_{N_k-1}}\right) \\ &= \text{Diag}(\boldsymbol{\beta}) \otimes I, \end{aligned}$$

where $\otimes$ is the Kronecker product [11].

Using (5) in (2), the model which includes the vector of phase errors $\boldsymbol{\beta}$ is

$$\boldsymbol{d} = F(\boldsymbol{\beta})\boldsymbol{g} + \boldsymbol{\eta}. \quad (6)$$

3.0 Proposed Autofocus Method Derivation

If the residual phase is not compensated for, the resulting formed image will not be in focus and will have poor contrast. What the proposed method provides is a vector $\hat{\boldsymbol{\beta}}$ of phase correction terms such that $[\hat{\boldsymbol{\beta}}]_i = \hat{\beta}_i$, which is an estimate of β_i.

The proposed method for estimating $\boldsymbol{\beta}$ uses subspace fitting principles that are well known in array processing literature [12]. In [10], solving for the ML ground reflectivity estimates reduces to

$$\text{minimize} \quad J(\boldsymbol{g}) = \|F\boldsymbol{g} - \boldsymbol{d}\|_2^2.$$

Using (6) we can alter the minimization problem to include the phase error vector

$$\text{minimize} \quad J(\boldsymbol{g}, \boldsymbol{\beta}) = \|F(\boldsymbol{\beta})\boldsymbol{g} - \boldsymbol{d}\|_2^2 \text{ subject to } |\beta_i| = 1. \quad (7)$$

Equation (7) can be minimized with respect to $\boldsymbol{g}$ and $\boldsymbol{\beta}$ separately. Solving first for $\boldsymbol{g}$ gives

$$\boldsymbol{g} = (F(\boldsymbol{\beta})^H F(\boldsymbol{\beta}))^{-1} F(\boldsymbol{\beta})^H \boldsymbol{d}. \quad (8)$$

Substituting (8) into (7), the problem becomes

$$\text{minimize} \quad J_1(\boldsymbol{\beta}) = \left\|(I - P_{F(\boldsymbol{\beta})})\boldsymbol{d}\right\|_2^2 \text{ subject to } |\beta_i| = 1. \quad (9)$$

Expanding the norm, using equation (5), and recognizing the form of the resulting equation, the minimization of $J_1(\boldsymbol{\beta})$ with respect to $\boldsymbol{\beta}$ is equivalent to maximizing the following

$$\hat{\boldsymbol{\beta}} = \arg\max_{\boldsymbol{\beta}} \boldsymbol{d}^H \Lambda_{\boldsymbol{\beta}} F(F^H F)^{-1} F^H \Lambda_{\boldsymbol{\beta}}{}^H \boldsymbol{d} \text{ subject to } |\beta_i| = 1. \quad (10)$$

Because $\Lambda_{\boldsymbol{\beta}}$ is a diagonal matrix, its diagonal and $\boldsymbol{d}$ can be swapped

$$\Lambda_{\boldsymbol{\beta}}{}^H \boldsymbol{d} = \Lambda_{\boldsymbol{d}} I_1 \boldsymbol{\beta}^*,$$

where $I_1 = I \otimes \mathbf{1}$. Substituting this result into (10) and using (3) gives

$$\hat{\boldsymbol{\beta}} = \arg\max_{\boldsymbol{\beta}} \boldsymbol{\beta}^T M \boldsymbol{\beta}^* \text{ subject to } |\beta_i| = 1, \quad (11)$$

where $M = G^H (F^H F)^{-1} G$ and G is defined in (4).

It is important to note that the optimization in (11) is not as simple as finding the eigenvector associated with the largest eigenvalue of M because this method does not capture the constraint that $|\beta_i| = 1$. From (11) it is apparent that the image does not have to be formed in order to estimate $\boldsymbol{\beta}$.

4.0 Optimization Method

Using the definition of β_i, the constrained optimization problem in (11) can be re-stated as the following unconstrained problem

$$\text{maximize} \quad J(\boldsymbol{\phi}) = e^{j\boldsymbol{\phi}^T} M e^{-j\boldsymbol{\phi}}, \quad (12)$$

where $\left[e^{\pm j\boldsymbol{\phi}}\right]_i = e^{\pm j\phi_i}$. The unconstrained formulation in (12) can be optimized by gradient ascent. The gradient of the unconstrained objective is

$$\frac{\partial J(\boldsymbol{\phi})}{\partial \boldsymbol{\phi}} = 2\Re\{j\text{Diag}(e^{j\boldsymbol{\phi}})Me^{-j\boldsymbol{\phi}}\}.$$

The update rule for gradient ascent is

$$\boldsymbol{\phi}_{n+1} = \boldsymbol{\phi}_n + \mu \frac{\partial J(\boldsymbol{\phi})}{\partial \boldsymbol{\phi}},$$

where μ is the step-size parameter and can be either fixed or found from a line search. The gradient ascent can be initialized with $\boldsymbol{\phi}_n = \mathbf{0}$, which assumes there are no phase errors initially.

Each iteration of this method has low computational complexity. However, many iterations are required for good estimates.

5.0 Results of Proposed Method

This section demonstrates the proposed autofocus method on simulated data. The original image has three strong reflectors in a background of weaker Gaussian distributed reflectors. The original image is illustrated in figure 1. The simulated data has the sinusoidal phase error illustrated in figure 2. Figure 3 illustrates the CBP reconstruction without any phase correction. Figure 4 compares the estimates found after 100,000 iterations of gradient ascent with a fixed step-size $\mu = 1.3 \times 10^{-7}$ to the original phase error. Finally, figure 5 illustrates the CBP reconstruction after applying the phase error estimates.

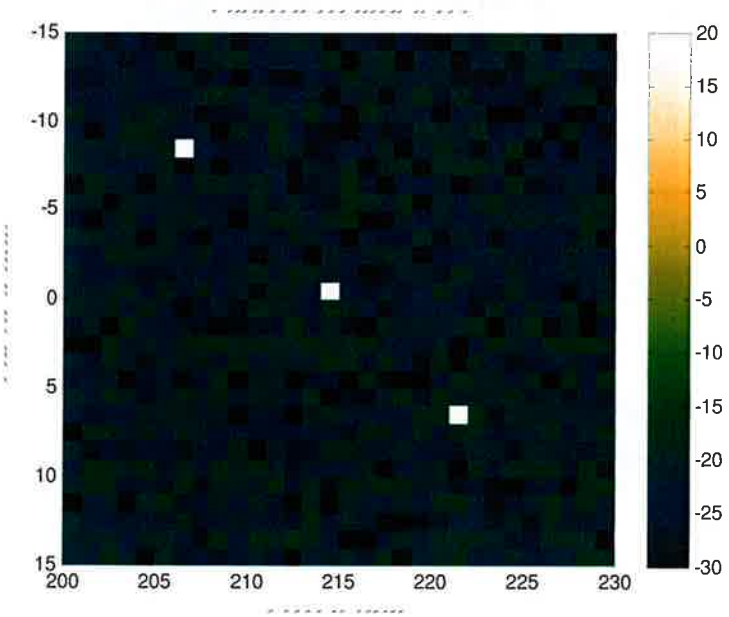

Figure 1: Original Image

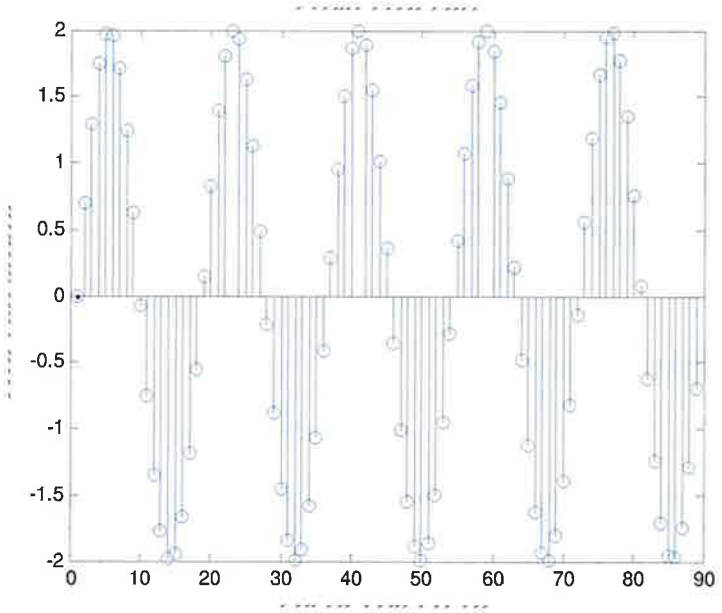

Figure 2: Applied Phase Error

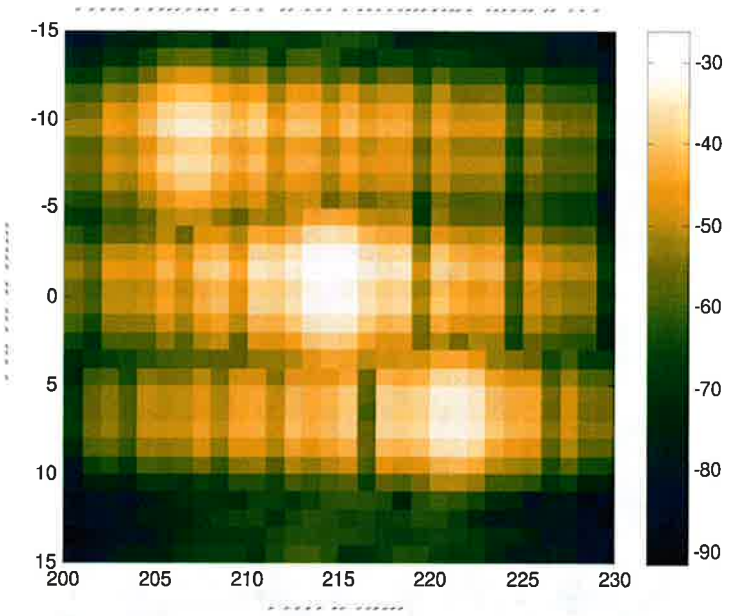

Figure 3: CBP Reconstruction Without Phase Compensation

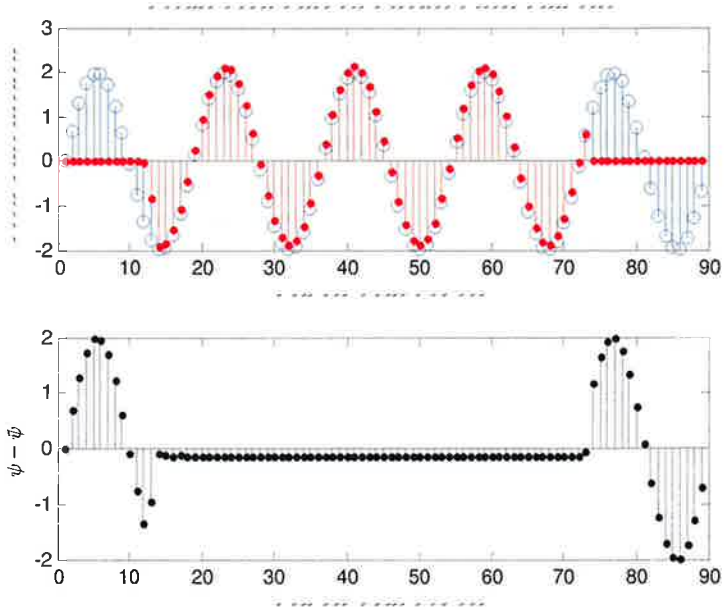

Figure 4: Phase Error Estimates vs. Applied Phase Error (Top); Error Between the Applied and Estimated Phase Error (Bottom)

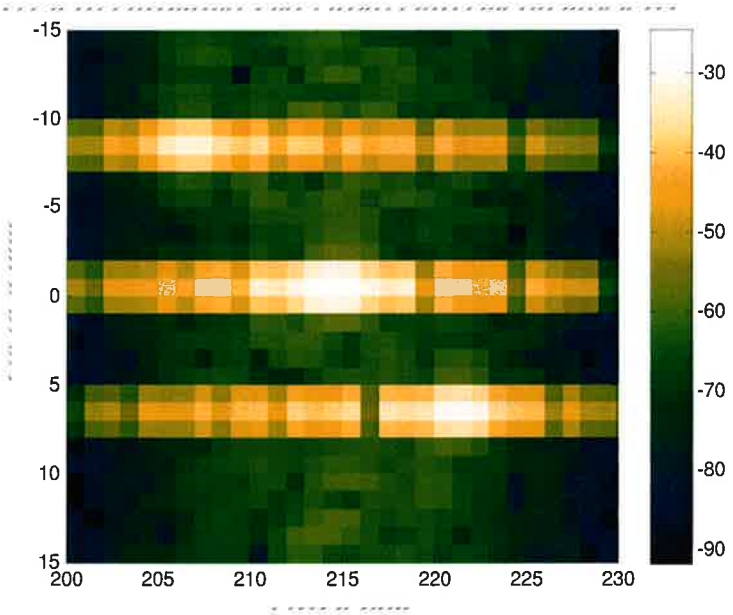

Figure 5: CBP Reconstruction With Phase Error Compensation

6.0 Discussion of Results

It is clear that the CBP image reconstructed using the phase error estimates is more focused than the CBP image without phase error compensation. It is interesting to note that after 100,000 iterations the phase estimates in figure 4 are off by a constant phase from about pulse 14 to pulse 74 and that virtually no phase estimates are made for the first and last set of pulses.

The constant phase error difference from pulses 14 to 74 do not affect the quality of the resulting image because it is the magnitude of the reflectivity that is being displayed. The first and last set of pulses obtain very poor estimates because of the lack of data that support the phase estimation in those regions. Phase estimates in these regions will eventually be obtained if the simulation is allowed to run long enough.

The gradient ascent method obtains good estimates fairly quickly in the regions where there is a lot of data (or strong reflectors) to support the estimates.

7.0 Conclusion

This paper proposed a model-based autofocus method for stripmap SAR. It was shown that the phase error estimates obtained from the proposed method can be applied to the data while simultaneously forming the image via the CBP algorithm.

Well known subspace fitting principles were used to obtain the optimization problem for the autofocus method. It was shown that the optimization problem could be solved using the gradient ascent method.

A simulated example was given to demonstrate that the phase error estimates can be obtained without forming the image. Hence, the proposed autofocus method is non-iterative in the sense that iterations between the image and range compressed domains are not needed to obtain the phase estimates, as is common in other autofocus methods.

Future work in this area include: exploring other optimization methods, determining a method for obtaining phase error estimates in a user selected region of interest, and exploring the idea of reducing the problem size by estimating a decimated phase error vector (provided the phase error is band-limited 'enough' with respect to the pulse repetition frequency) and interpolating the result to obtain the full phase error history.

8.0 Acknowledgements

The authors would like to thank the Space Dynamics Laboratory located in Logan, Utah for their support in this effort.

9.0 References

[1] R. Morrison, M. Do, and D. Munson, "MCA: A multichannel approach to SAR autofocus," *Image Processing, IEEE Transactions on*, vol. 18, no. 4, pp. 840 –853, 2009.

[2] J. C. Jakowatz, D. E. Wahl, P. H. Eichel, D. C. Ghiglia, and P. A. Thompson, *Spotlight-mode Synthetic Aperture Radar: A Signal Processing Approach*. New York: Springer, 1996.

[3] P. Samczynski and K. Kulpa, "Coherent mapdrift technique," *Geoscience and Remote Sensing, IEEE Transactions on*, vol. 48, no. 3, pp. 1505 – 1517, 2010.

[4] T. Calloway and G. Donohoe, "Subaperture autofocus for synthetic aperture radar," *Aerospace and Electronic Systems, IEEE Transactions on*, vol. 30, pp. 617 –621, Apr. 1994.

[5] J. Wang and X. Liu, "SAR minimum-entropy autofocus using an adaptive-order polynomial model," *Geoscience and Remote Sensing Letters, IEEE*, vol. 3, no. 4, pp. 512 –516, 2006.

[6] J. Morrison, R.L. and M. Do, "A multichannel approach to metric based SAR autofocus," in *Image Processing, 2005. ICIP 2005. IEEE International Conference on*, vol. 2, pp. II – 1070–3, 2005.

[7] J. C. V. Jakowatz and D. E.Wahl, "Eigenvector method for maximum likelihood estimation of phase errors in synthetic-aperture-radar imagery," *J. Opt. Soc. Am. A*, vol. 10, 12 1993.

[8] F. Berizzi, G. Corsini, M. Diani, and M. Veltroni, "Autofocus of wide azimuth angle SAR images by contrast optimisation," in *Geoscience and Remote Sensing Symposium, 1996. IGARSS '96. 'Remote Sensing for a Sustainable Future.', International*, vol. 2, pp. 1230 –1232 vol.2, May 1996.

[9] R. Morrison, M. N. Do, and D. Munson, "SAR image autofocus by sharpness optimization: A theoretical study," *Image Processing, IEEE Transactions on*, vol. 16, no. 9, pp. 2309 –2321, 2007.

[10] R. D. West, J. H. Gunther, and T. K. Moon, "Maximum likelihood estimation of ground reflectivity from synthetic aperture radar data," in *56th Annual Meeting of the MSS Tri-Services Radar Symposium*, (Orlando, FL), SENSIAC, June 2010.

[11] T. K. Moon and W. C. Stirling, *Mathematical Methods and Algorithms for Signal Processing*. Prentice Hall, 2000.

[12] M. Viberg and B. Ottersten, "Sensor array processing based on subspace fitting," *Signal Processing, IEEE Transactions on*, vol. 39, pp. 1110 – 1121, May 1991.